

# PPJudge: Towards Human-Aligned Assessment of Artistic Painting Process

Shiqi Jiang  
East China Normal University  
Shanghai, China  
52265901032@stu.ecnu.edu.cn

Xinpeng Li  
East China Normal University  
Shanghai, China  
51275901118@stu.ecnu.edu.cn

Xi Mao  
East China Normal University  
Shanghai, China  
xmao@design.ecnu.edu.cn

Changbo Wang  
East China Normal University  
Shanghai, China  
cbwang@cs.ecnu.edu.cn

Chenhui Li\*  
East China Normal University  
Shanghai, China  
chli@cs.ecnu.edu.cn

## ABSTRACT

Artistic image assessment has become a prominent research area in computer vision. In recent years, the field has witnessed a proliferation of datasets and methods designed to evaluate the aesthetic quality of paintings. However, most existing approaches focus solely on static final images, overlooking the dynamic and multi-stage nature of the artistic painting process. To address this gap, we propose a novel framework for human-aligned assessment of painting processes. Specifically, we introduce the Painting Process Assessment Dataset (PPAD)—the first large-scale dataset comprising real and synthetic painting process images, annotated by domain experts across eight detailed attributes. Furthermore, we present PPJudge (Painting Process Judge), a Transformer-based model enhanced with temporally-aware positional encoding and a heterogeneous mixture-of-experts architecture, enabling effective assessment of the painting process. Experimental results demonstrate that our method outperforms existing baselines in accuracy, robustness, and alignment with human judgment, offering new insights into computational creativity and art education.

## CCS CONCEPTS

• Computing methodologies → Computer vision tasks; • Applied computing → Fine arts.

## KEYWORDS

Painting assessment, Painting dataset, Deep learning, Fine arts

## ACM Reference Format:

Shiqi Jiang, Xinpeng Li, Xi Mao, Changbo Wang, and Chenhui Li. 2025. PPJudge: Towards Human-Aligned Assessment of Artistic Painting Process. In *Proceedings of (ACM MM) Proceedings of the 33rd ACM International*

\*Corresponding author.

Permission to make digital or hard copies of all or part of this work for personal or classroom use is granted without fee provided that copies are not made or distributed for profit or commercial advantage and that copies bear this notice and the full citation on the first page. Copyrights for components of this work owned by others than the author(s) must be honored. Abstracting with credit is permitted. To copy otherwise, or republish, to post on servers or to redistribute to lists, requires prior specific permission and/or a fee. Request permissions from permissions@acm.org.

ACM MM, 2025, Dublin, Ireland

© 2025 Copyright held by the owner/author(s). Publication rights licensed to ACM.  
ACM ISBN 978-x-xxxx-xxxx-x/YY/MM  
<https://doi.org/XXXXXXX.XXXXXXX>

*Conference on Multimedia (MM'25), October 27-31, 2025, Dublin, Ireland.*  
ACM, New York, NY, USA, 9 pages. <https://doi.org/XXXXXXX.XXXXXXX>

## 1 INTRODUCTION

In recent years, with the rapid development of computer vision and generative models, intelligent assessment has shown great potential in the field of art. In painting-related research, existing painting aesthetic assessment methods [22, 23, 47] are capable of evaluating static artworks from dimensions such as composition, color, and style, thereby advancing computational understanding of visual aesthetics. However, in the context of art education, painting is regarded as a multi-stage dynamic practice that involves observation, ideation, composition, and execution [6, 8]. Therefore, the assessment of the painting process is particularly crucial, as it more accurately reflects the painter's abilities in observation, reasoning, and execution. By analyzing quantitative attributes such as stability and reasoning depth [7], researchers can obtain a more comprehensive understanding of a painter's artistic ability.

Traditionally, the assessment of the painting process has been conducted by experts in art or design, who evaluate factors such as consistency, stability, and reasoning depth throughout the process to infer the artist's level. However, this approach is inherently time-consuming and may be influenced by personal biases or preconceived notions. With the recent development of generative models, researchers have begun reconstructing human painting processes using diffusion-based approaches [34]. While these methods [27, 37] can serve as useful references for understanding the painting process, they cannot be regarded as definitive standards. This is because their training objectives focus primarily on consistency with the final outcome, without any direct supervision of the intermediate steps. As a result, the generated painting processes often follow fixed patterns and lack the diversity and creativity characteristic of genuine human creation.

Recently, researchers have employed multimodal models to tackle tasks related to painting assessment [5, 24]. However, these approaches face two major challenges when applied to painting process assessment. First, there is currently no annotated dataset specifically designed for this task. Existing datasets [22, 24] focus on evaluating the content of the final image, rather than the painting process. Second, current assessment models typically operate on a single image and are not designed to handle multi-image inputs that represent a sequence of painting steps.

To overcome existing challenges, we introduce a dataset specifically designed for painting process assessment: the Painting Process Assessment Dataset (PPAD). It consists of approximately 15,000 real paintings and 10,000 synthetic paintings, each annotated by domain experts. To the best of our knowledge, PPAD is the first dataset dedicated to studying and evaluating the painting process. In addition, we propose PPJudge (Painting Process Judge), which effectively leverages both category-level and process-level features of a given painting. PPJudge is a significant extension of the Transformer architecture with Mixture-of-Experts (MoE) modules. First, we introduce an angular correction mechanism in positional encoding, enabling the model to better capture the sequential nature of painting. Second, we employ a heterogeneous MoE architecture, where experts differ in depth, allowing the model to adaptively select appropriate experts based on different levels of attributes in the painting process. Furthermore, we constrain the shared expert modules by painting categories, ensuring the evaluation is context-aware and category-sensitive.

In summary, our main contributions are as follows:

- We address the underexplored problem of painting process assessment and introduce a new dataset, PPAD, consisting of about 15,000 real and 10,000 synthetic paintings, each with expert annotations.
- We propose a novel Painting Process Assessment Model called PPAM, which incorporates temporal-aware position encoding and a heterogeneous MoE architecture.
- Extensive experiments on PPAD demonstrate the superior performance of our model in assessing the quality of painting processes.

## 2 RELATED WORK

### 2.1 Painting Assessment Dataset

In earlier years, [46] annotated 500 abstract paintings by rating them on a Likert scale of 1-7 to assess emotional valence. To explore the impact of subjectivity on the evaluation of paintings, JenAesthetics [1] includes 1,628 oil paintings along with results from a subjective study. Furthermore, JenAesthetics $\beta$ [2] extends this dataset by adding 281 high-quality paintings and analyzing various factors influencing painting assessment. Building upon these, VAPS[17] comprises 999 paintings spanning five genre categories. WikiArt<sup>1</sup> is a widely used painting dataset that contains 81,449 artworks, annotated with 27 styles and 45 genres. Similar to WikiArt, Art500k [30] includes over 500K artistic images, each labeled with more than 10 attributes. OmniArt [38] is a large-scale dataset with over one million artworks, providing a rich annotation structure. SemArt [18] is a multi-modal dataset for semantic art understanding, containing 21,383 paintings with detailed metadata. More recently, BAID [47] is introduced, comprising 60,337 artistic images across various art forms, with more than 360,000 user-contributed votes for aesthetic evaluation. AACP dataset [22] contains 21,200 children's paintings, including 20,000 unlabeled paintings generated by DALL-E [33] and 1,200 expert-annotated paintings.

Unlike the painting datasets mentioned above, the dataset we constructed is specifically designed to capture the painting process.

It contains both real and AI-generated data, all of which have been expertly labeled with multiple attributes.

### 2.2 Painting Assessment Model

Unlike image aesthetics assessment (IAA) models, which have developed rapidly thanks to large-scale IAA datasets, painting assessment models have progressed at a slower pace. Early painting assessment models focused on classifying paintings into styles or genres [9, 25, 36, 40]. With the advancement of multimodal models, many studies have started to explore painting evaluation using multimodal approaches. CLIP-Art [12] utilizes CLIP [32] to encode paintings into embeddings for downstream tasks. Additionally, SAAN [47] introduces style-specific and generic aesthetic features via spatial information fusion for painting assessment. AACP [22] introduces synthetic paintings through a self-supervised learning strategy to address the challenge of insufficient painting annotations, marking the first use of synthetic data in painting evaluation. Recently, GalleryGPT [5] fine-tunes a multimodal large language model to generate formal analyses for paintings. ArtCLIP [24] proposes a multi-attribute contrastive learning framework for painting assessment across multiple categories and attributes.

In this paper, we aim to evaluate the painting process rather than the final painting. Unlike previous methods that map a painting to one or more scores, our method processes multiple paintings simultaneously and analyzes differences across different stages of the painting process.

### 2.3 Sequence Image Representation

Sequence image representation has evolved significantly over the past decades, covering both image and video domains. Convolutional neural networks (CNNs) were long the dominant architecture for visual representation learning [19, 20]. With the rise of Transformer-based models [14], vision transformers (ViTs) have become popular image encoders. DeiT [44] introduces knowledge distillation to enable data-efficient ViT training, while Swin Transformer [28] proposes hierarchical attention with local windows for improved efficiency and scalability. To further enhance image encoders, researchers explore sparse and lightweight architectures. Switch Transformers [15] introduces sparse routing to reduce computation, which is widely adopted in large-scale models [13, 41].

Compared to image encoders, video encoders additionally capture temporal dynamics across frames. Early approaches extended 2D CNNs to 3D to model spatial and temporal features [10]. Slow-Fast Networks [16] introduces dual pathways to capture both slow and fast temporal patterns. Recently, many works have adapted Transformers to video understanding. ViViT [3] proposes factorized attention strategies for efficient spatio-temporal modeling, while TimeSformer [4] decouples spatial and temporal attention to reduce complexity. Video Swin Transformer [29] extends hierarchical attention to the temporal dimension. Self-supervised video pretraining has also gained attention. VideoMAE [43, 45] leverages masked video modeling to learn strong temporal-spatial representations from unlabeled videos.

Image encoders process sequential images by simply aggregating the embeddings of individual frames, which fails to effectively capture inter-frame relationships. In contrast, video encoders model

<sup>1</sup><https://www.wikiart.org/>

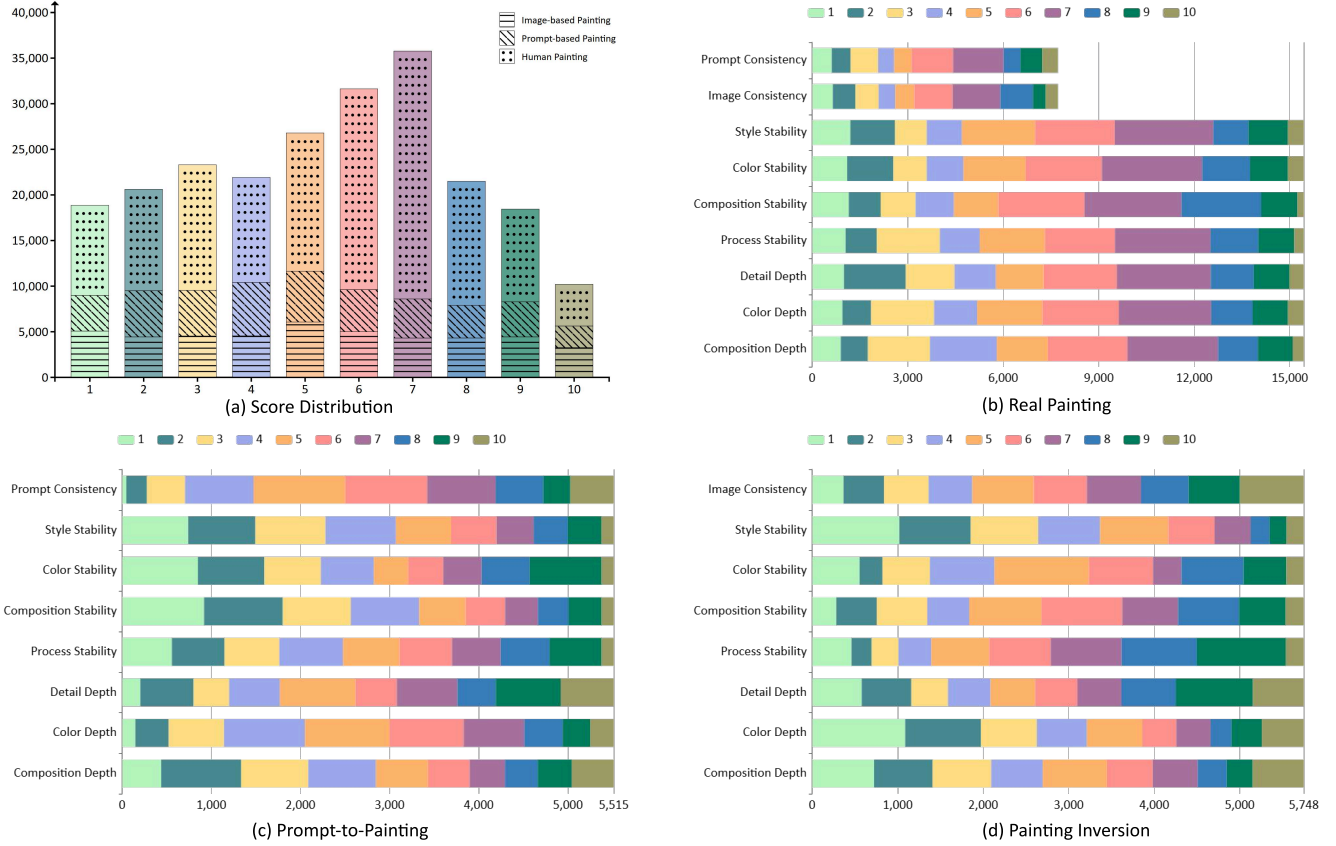


**Figure 1: Statistics of our dataset. (a) shows the distribution of scores for paintings from different sources. (b), (c), and (d) show the distribution of painting attributes from real paintings, prompt-to-painting generation, and painting inversion, respectively.**

temporal dynamics but require re-encoding the entire frame sequence at each step, making real-time assessment impractical. In this paper, we propose an efficient design based on an image encoder augmented with key-value caching. Our method supports incremental updates, avoiding redundant computation and significantly improving inference efficiency.

### 3 DATASET

Our Painting Process Assessment Dataset (PPAD) consists of pairs  $(R_m, P_m)$ , where  $R_m$  denotes the  $m$ -th reference painting or prompt, and  $P_m = \{P_{m1}, P_{m2}, \dots, P_{mn}\}$  represents a sequence of  $n$  paintings corresponding to  $R_m$ . We first collect a large number of real-world painting process images (Section 3.1). To improve the generalization ability of models, we further introduce synthetic painting process images (Section 3.2). Finally, we invite domain experts to evaluate the painting processes using eight attributes (Section 3.3).

#### 3.1 Painting Collection

Following [22] and [26], we recruit hundreds of art and drawing majors as participants aged between 22 and 30. Before painting, each participant is given either a random prompt or a reference painting. Participants can create freely based on the prompt or replicate the reference as faithfully as possible. The entire painting

process is recorded as a video focused solely on the canvas. Since participants often pause to observe or think, the videos contain many redundant frames with little visual change. Moreover, painting durations vary significantly across individuals. To address these issues, we first downsample the video by extracting one frame every  $k$  frames. We then compute the visual difference between consecutive frames based on pixel-wise L2 distance. A frame is selected as a key frame if its visual difference from the last selected key frame exceeds a threshold  $\tau$ . To adapt to varying painting speeds and session durations, we dynamically adjust  $\tau$  based on the total visual change across the video. Finally, we enforce minimum and maximum limits on the number of extracted key frames to ensure consistent representation quality.

After filtering out invalid and incomplete paintings, we collected approximately 15,000 paintings, 80% of which are allocated for training and the remaining 20% for testing.

#### 3.2 Dataset Expansion

To improve the generalization ability of the model, we introduce synthetic data. Early painting reconstruction efforts, such as [21], were inspired by human painters and trained using reinforcement learning. Later, [48] and [27] used a stroke-based rendering approach to improve the stability of painting reconstruction. However,

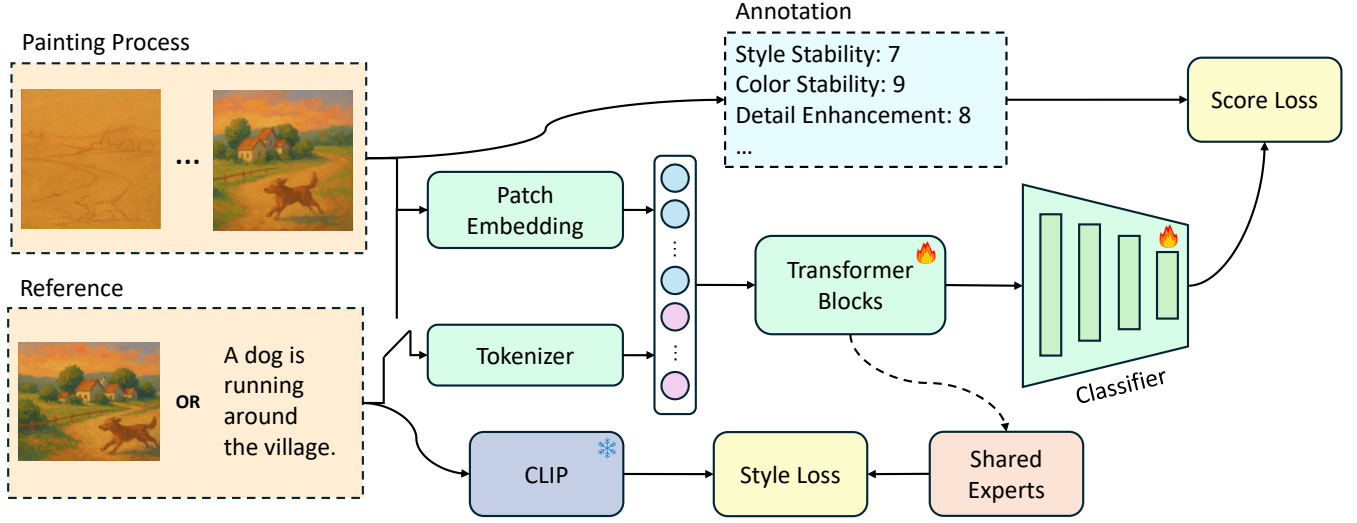


**Figure 2: Pipeline of our model.** Process images and a reference (either an image or a prompt) are first embedded into token representations. Improved transformer blocks extract features of the painting process, with a style loss guiding the shared experts toward capturing stylistic characteristics. The extracted features are then mapped to assessment scores by a classifier. The transformer blocks and the classifier are jointly optimized with a score loss.

the paintings reconstructed by such methods exhibit significant differences from the target paintings. Recently, diffusion-based models [34] have achieved great success. Therefore, [11, 37, 42] have leveraged diffusion models to generate high-quality process images.

In this paper, we obtain synthetic data in two ways. First, we use ProcessPainter [37] to generate about 5,000 paintings along with process images from prompts. These prompts are simple descriptions of themes or scenes, with no painting style specified. Second, we use Paints-Undo [42] to invert real paintings to obtain about 5,000 process images. 90% of the synthetic data is used to pre-train our models, while the remaining 10% is used for testing.

### 3.3 Painting Annotation

Fifteen experts in the field of art are invited to evaluate the paintings. Based on fundamental drawing principles and design theory, the experts divided painting process assessment into three aspects: *Painting Consistency*, *Painting Stability*, and *Painting Depth*.

**Painting Consistency** (Consis.) evaluates whether the final painting accurately reflects the core themes and elements of the given prompt or reference image, maintaining strong semantic and visual similarity. A higher score indicates stronger alignment between the final painting and the reference.

**Painting Stability** evaluates the smoothness and coherence of transitions during the painting process. This attribute is assessed across four dimensions: *style*, *color*, *composition*, and *process*. Style stability (S. S.) refers to whether the sequence maintains a consistent artistic style without abrupt or inconsistent changes; Color stability (Col. S.) assesses whether the color transitions are gradual and harmonious, avoiding sudden or jarring shifts such as the appearance of unnatural hues; Composition stability (Com. S.) considers whether the visual focus or layout changes drastically across frames; Process stability (Proc. S.) evaluates whether the painting

progresses smoothly without excessive corrections, regressions, or unnecessary modifications.

**Painting Depth** assesses whether the painting process exhibits progressive refinement through the gradual introduction of new techniques or complex visual elements (e.g., color schemes, composition, and light-shadow treatments). This aspect is evaluated in terms of *detail*, *color*, and *composition*. Detail depth (D. D.) measures the incremental enrichment of visual details and their contribution to expressive power; Color depth (Col. D.) evaluates whether the use of color becomes more sophisticated over time, enhancing visual impact; Composition depth (Com. D.) assesses whether compositional structures grow in complexity and contribute to the overall visual richness.

In total, the painting process is assessed using eight attributes on a scale from 1 to 10. Specifically, each painting’s drawing process is evaluated by multiple experts, and each attribute receives multiple scores. The final score for each attribute is computed as the average of these scores. This approach helps mitigate the impact of subjectivity in the evaluation process.

## 4 METHOD

### 4.1 Overall Architecture

The assessment of the painting process can be represented as  $Scores = M(P_m|R_m)$ , where  $M$  denotes the model. Our model consists of transformer blocks and a classifier. The overall structure of the transformer block is shown in Figure 3. To adapt the model to 2D patches extracted from sequential images, we apply an angular adjustment to the original rotary positional encoding (Section 4.2). Next, to allow the model to adapt to different types of paintings and better disentangle painting features, we propose a heterogeneous mixture of experts (Section 4.3). Finally, we describe our classifier and the loss function in Section 4.4.

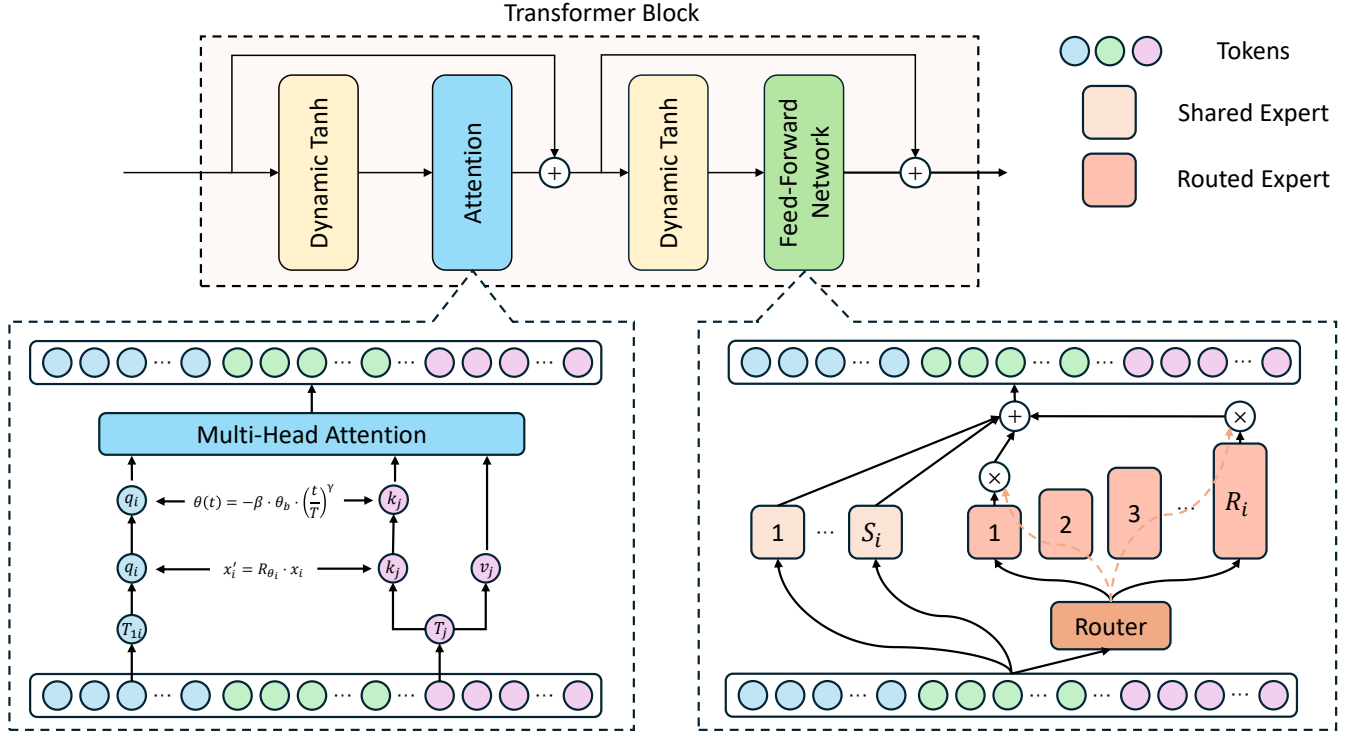


Figure 3: Illustration of the basic architecture of our transformer blocks.

## 4.2 Positional Encoding

Rotary Position Embedding (RoPE) [39] is widely used in multi-modal large language models [31, 41]. RoPE improves generalization by mapping token representations into a high-dimensional rotational space, which can be formalized as:

$$\alpha_{ij}^{RoPE} = q_i R(i-j) k_j^T, \quad (1)$$

where  $q_i = W_Q(x_i)$  is the query vector from the  $i$ -th token, and  $k_j = W_K(x_j)$  is the key vector from the  $j$ -th token.  $R(i-j)$  is a block diagonal matrix that applies a position-dependent rotation to the query and key vectors.

However, this approach is not well-suited for sequential image modeling, where spatial relationships between tokens should be preserved. Given an  $n$ -step sequence of paintings  $P = \{p_1, \dots, p_n\}$ , it is tokenized into  $T = \{\{t_{11}, \dots, t_{1m}\}, \dots, \{t_{n1}, \dots, t_{nm}\}\}$ . Although  $t_{21}$  and  $t_{11}$  occupy the same spatial location in adjacent frames, their positions in the flattened token sequence are far apart, resulting in exaggerated angular separation under standard RoPE.

To correct for this discrepancy, we introduce a time-dependent correction term, with later frames receiving more negative corrections, and earlier frames having values closer to zero to mitigate temporal angular drift. Formally, given the standard RoPE rotation matrix parameterized by position  $p$ , we introduce a temporal adjustment to the rotation angle as:

$$\theta_{\text{time}}(t) = -\beta \cdot \theta_{\text{base}} \cdot \left(\frac{t}{T}\right)^\gamma, \quad (2)$$

where  $t$  is the time step,  $T$  is the total number of time steps,  $\theta_{\text{base}} = \theta_{\text{RoPE}}(p=0)$  is the baseline rotation angle at the first spatial token,  $\beta$  is a tunable factor controlling the degree of temporal correction, and  $\gamma$  is an optional smoothing exponent that adjusts the rate of temporal decay.

## 4.3 Heterogeneous Mixture of Experts

MoE offers advantages in terms of faster convergence and improved computational efficiency by leveraging sparse activation. In multi-attribute prediction tasks, using a single FFN often results in feature entanglement [22], making the learning process slower and reducing generalization. MoE mitigates this issue by dynamically selecting specialized experts, thereby enhancing both learning efficiency and model robustness.

In painting process assessment, different visual attributes require features at varying levels of abstraction. For example, color-related attributes often depend on shallow features, while composition-related attributes require deeper, more global representations. To accommodate these heterogeneous needs, we design a heterogeneous MoE architecture, as shown in Figure 3. Similar to [13], our MoE consists of two types of experts: shared and routed. The shared experts are conditioned on the painting style, which plays an essential role in shaping the painting process. We leverage CLIP [32] embeddings to provide semantic supervision for style-aware shared experts. The routed experts are selected dynamically by a router and exhibit varying depths, allowing them to specialize in different attribute types. This design enables the model to process diverse artistic attributes in a more targeted and efficient manner.

**Table 1: Comparison of AANSPS, SAAN, ArtCLIP and ours on PPAD.**

Attribute	AACP				SAAN				ArtCLIP				Ours			
	SRCC	PCC	MSE	ACC	SRCC	PCC	MSE	ACC	SRCC	PCC	MSE	ACC	SRCC	PCC	MSE	ACC
Consis.	0.58	0.60	0.24	0.84	0.68	0.68	0.40	0.75	0.76	0.75	0.37	0.71	<b>0.78</b>	<b>0.79</b>	<b>0.12</b>	<b>0.92</b>
S. S.	0.49	0.47	0.42	0.73	0.65	0.61	0.53	0.79	0.67	0.59	0.35	0.83	<b>0.66</b>	<b>0.65</b>	<b>0.22</b>	<b>0.85</b>
Col. S.	0.62	0.61	0.22	0.81	0.64	0.71	0.38	0.81	0.65	0.70	0.46	0.58	<b>0.75</b>	<b>0.78</b>	<b>0.11</b>	<b>0.89</b>
Com. S.	0.64	0.63	0.23	0.82	0.64	0.68	0.33	0.75	0.52	0.45	0.52	0.88	<b>0.77</b>	<b>0.75</b>	<b>0.16</b>	<b>0.90</b>
Proc. S.	0.60	0.64	0.30	0.72	0.69	0.68	0.45	0.75	0.63	0.64	0.35	0.79	<b>0.70</b>	<b>0.73</b>	<b>0.16</b>	<b>0.85</b>
D. D.	0.59	0.61	0.34	0.69	0.47	0.49	0.65	0.63	0.69	0.76	0.27	0.75	<b>0.74</b>	<b>0.73</b>	<b>0.14</b>	<b>0.87</b>
Col. D.	0.62	0.65	0.30	0.73	0.67	0.66	0.26	0.78	0.60	0.59	0.18	0.75	<b>0.69</b>	<b>0.68</b>	<b>0.20</b>	<b>0.86</b>
Com. D.	0.59	0.56	0.29	0.71	0.47	0.49	0.70	0.67	0.66	0.72	0.31	0.71	<b>0.80</b>	<b>0.76</b>	<b>0.13</b>	<b>0.91</b>

#### 4.4 Classifier and Loss Function

The classifier maps the model output to the scores. Unlike AACP, our backbone already has the ability to decouple features. Following Laion’s aesthetic score predictor [35], we use a multi-layer MLP as the classifier.

During training, we use two loss functions: style loss and score loss. The style loss is meant to constrain the sharing expert to learn style-specific features. First, we use a pre-trained CLIP model to distinguish between different types of paintings, which can be expressed as:

$$t^* = \arg \max_{t \in T} \frac{E_p \cdot t}{\|E_p\| \|t\|}, \quad (3)$$

where  $T$  represents a set of text embeddings, where each text is of the form "This is a {style} painting.", and  $E_p$  denotes the reference image embedding. We set  $E_{style} = t^*$ . Second, the output of the shared experts is projected into the style dimension using a projection module, which can be expressed as:

$$E_{se}^l = W_{proj} \cdot O_{se}^l, \quad (4)$$

where  $W_{proj}$  is the learnable projection matrix and  $O_{se}^l$  represents the output of the shared expert at layer  $l$ . We use cosine similarity loss to calculate the style loss, which can be expressed as:

$$L_{style}^l = 1 - \frac{E_{style} \cdot E_{se}^l}{\|E_{style}\| \|E_{se}^l\|}. \quad (5)$$

Finally, the total style loss is defined as:

$$L_{style} = \sum_{l=1}^L \alpha_l \cdot L_{style}^l, \quad (6)$$

where  $\alpha_l$  is the weighting coefficient for layer  $l$ .

The score loss is calculated using the Mean Squared Error (MSE), which can be expressed as:

$$L_{score} = \frac{1}{n} \sum_{i=1}^n (y_{score}^{(i)} - \hat{y}_{score}^{(i)})^2, \quad (7)$$

where  $n$  denotes the number of attributes.

Therefore, the total loss can be expressed as:

$$L_{total} = L_{style} + \lambda_{score} L_{score}, \quad (8)$$

where  $\lambda_{score}$  is a weighting coefficient to balance the style loss and score loss.

## 5 EXPERIMENT

### 5.1 Experiment Setting

We set the number of Transformer blocks to 8. The classifier consists of a 3-layer MLP and uses the SiLU activation function. We set the hyperparameter  $\alpha$  in the loss function to increase with  $l$  from 0 to 0.8, following an exponential schedule. The weighting coefficient  $\lambda_{score}$  is set to 10. Our model is trained on 8 NVIDIA H800 GPUs with a batch size of 256. During the pre-training phase with synthetic data, we train the model for 200 epochs using the AdamW optimizer with a learning rate of  $1 \times 10^{-4}$ . In the subsequent training phase with real data, we employ the Adam optimizer with a learning rate of  $1 \times 10^{-5}$  and train for 20 epochs.

### 5.2 Metrics

To evaluate the performance of each model, we adopt three widely used metrics: 1) Spearman’s Rank Correlation Coefficient (SRCC), 2) Pearson Correlation Coefficient (PCC), and 3) Mean Squared Error (MSE). Additionally, we compute classification accuracy (ACC) by rounding both the predicted scores to the nearest integer and considering a prediction correct if the rounded values match.

### 5.3 Quantitative Experiment

We compare our method with several advanced painting assessment models, including AACP [22], SAAN [47], and ArtCLIP [24]. All models are retrained on our PPAD dataset using their recommended configurations. Since AACP, SAAN, and ArtCLIP are designed for single-image input and do not support multi-image sequences, we adapt them by averaging the embeddings of multiple images and feeding the aggregated feature into the classifier.

Figure 4 shows examples of our dataset and comparison results. From the prediction scores presented, our method is significantly more accurate than the other methods. As shown in Table 1, our method outperforms all baselines across all metrics and attributes, demonstrating superior capability in assessing the painting process.

Furthermore, we compare the inference performance of each model. All experiments are conducted on a single NVIDIA H800 GPU, with the number of input images for each painting process set to 10. As shown in Table 2, our method achieves the fastest inference time among all methods. This demonstrates the potential of our approach to provide real-time feedback to the artist during the painting process.





Figure 4: Examples from our testset. The top two rows are real paintings and the bottom two rows are synthesized paintings. The painting is based on Prompt or Reference image. We show the scores labeled by the experts as well as the scores predicted by painting assessment models.

Table 2: Comparison of inference performance.

Model	Parameter (M)	Time (s)
AACP	62.17	0.03
SAAN	30.82	0.06
ArtCLIP	149.62	0.04
<b>Ours</b>	<b>17.21</b>	<b>0.01</b>

Table 3: Ablation studies on model components.

Model	SRCC	LCC	MSE	ACC
Base	0.48	0.43	0.34	0.61
+ Angular Corrections	0.59	0.61	0.29	0.68
+ Variable length	0.67	0.66	0.19	0.82
+ Style Loss	0.74	0.73	0.16	0.88

## 5.4 Ablation Study

As shown in Table 3, we start with the base Transformer equipped with a standard MoE architecture and incrementally introduce new modules. The performance steadily improves with the addition of angular corrections in positional encoding, variable-length expert modules, and style loss.

Furthermore, we investigate the impact of the number of shared experts and the number of activated routing experts per token. In our experimental setup, each token has a hidden dimension of 512, and the total number of experts is set to 32. As shown in Table 4, we conduct five groups of ablation experiments and find that the model achieves near-optimal performance when using 2 shared experts

and 4 routing experts. Increasing the number of shared or routing experts beyond this point yields only marginal improvements.

Based on the previous results, we select the optimal expert configuration and further investigate the impact of expert depth heterogeneity under a fixed number of activated routed experts. As shown in Table 5, we compare four configurations: (1) A1, where all experts are 1-layer MLPs; (2) A2, where all experts are 2-layer MLPs; (3) A3, which includes six experts with varying depths from 1 to 5; and (4) Ours, a structured heterogeneous setting with 16 experts of depth 1, 6 of depth 2, 4 of depth 3, and 2 each of depths 4 and 5. Our configuration consistently achieves the best performance across all four evaluation metrics, demonstrating the effectiveness of incorporating structured depth diversity among routed experts.

**Table 4: Ablation study on the number of (Shared experts + Routed experts).**

Nums.	SRCC	LCC	MSE	ACC
1 + 2	0.65	0.63	0.27	0.80
2 + 2	0.71	0.69	0.21	0.85
2 + 4	<b>0.74</b>	0.73	<b>0.16</b>	0.88
2 + 6	0.73	0.73	0.17	<b>0.89</b>
4 + 4	<b>0.74</b>	<b>0.75</b>	0.17	<b>0.89</b>

**Table 5: Comparison of expert depth configurations with fixed number of activated routed experts (Top-4).**

Expert Depth	SRCC	LCC	MSE	ACC
A1	0.69	0.68	0.22	0.83
A2	0.71	0.68	0.23	0.82
A3	0.62	0.60	0.31	0.76
<b>Ours</b>	<b>0.74</b>	<b>0.73</b>	<b>0.16</b>	<b>0.88</b>

**Table 6: Effect of Synthetic Data on Model Performance.**

Data	SRCC	LCC	MSE	ACC
Real data	0.68	0.66	0.23	0.84
+ 50% Synthetic data	0.71	0.69	0.19	0.85
+ 50% Synthetic data	0.74	0.72	0.16	0.88

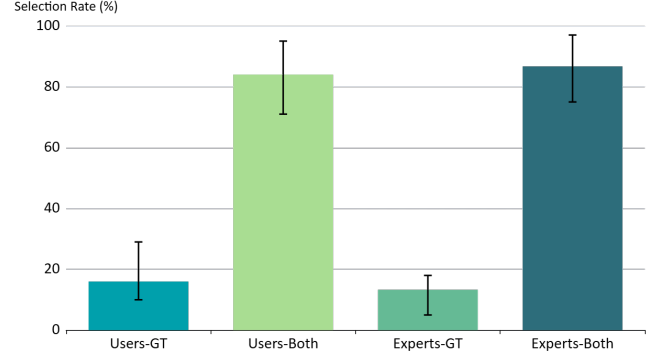
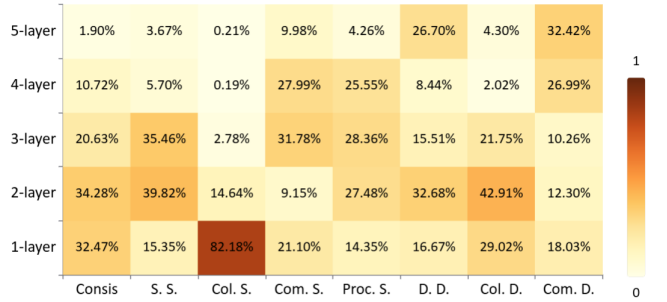
In addition, we analyze the impact of synthetic data on model performance. As shown in Table 6, the model achieves better results when synthetic data is progressively incorporated alongside real data, demonstrating the benefit of data augmentation in enhancing model generalization.

## 5.5 User Study

We invited ten participants with painting expertise and five art professionals to evaluate our results. Twenty painting sequences were randomly selected, each accompanied by the output generated by our model and the corresponding ground truth. The evaluators were asked to choose which result they preferred for each sequence, with the option to select both if they found them equally good. As shown in Figure 5, both regular participants and domain experts consistently preferred the assessment results produced by our model or considered them comparable to the ground truth. This demonstrates the human-aligned nature of our method from both professional and non-professional perspectives.

## 5.6 Visual Analysis

We visualize the internal routing behavior of our MoE model. We randomly select 1000 samples, and for each attribute, tokens with normalized contribution weights greater than 0.5 are identified as representative. We then analyze which experts these representative tokens are routed to in the final MoE layer. As shown in Figure 6, the

**Figure 5: Results of user study.****Figure 6: Heatmap of expert usage across different depths for each attribute.**

heatmap illustrates the expert usage frequency across different expert depths for each attribute. We observe that low-level attributes (e.g., color) tend to rely on shallower experts, while high-level attributes (e.g., composition) are routed to a broader range of expert depths. Overall, our MoE architecture exhibits balanced expert utilization and avoids the load imbalance issue, which contributes to improved model performance.

## 6 CONCLUSION

This paper addresses the challenging task of painting process assessment. To this end, we construct the PPAD dataset, which contains approximately 15,000 real paintings and 10,000 synthetic paintings, each annotated with eight attributes relevant to the painting process. Furthermore, we propose a novel model that incorporates time-aware angular correction in rotary positional encoding, along with hierarchical MoE modules enhanced by style awareness. Both quantitative experiments and user studies demonstrate that our method achieves state-of-the-art performance in painting process assessment. We also conduct ablation studies to evaluate the contribution of each component in our model.

In future work, we plan to further expand the scale and diversity of the PPAD dataset. Additionally, we aim to enrich the annotation of the painting process with linguistic descriptions, enabling a deeper understanding of the artist's skill level and providing more insightful feedback.



## REFERENCES

- [1] Seyed Ali Amirshahi, Gregor Uwe Hayn-Leichsenring, Joachim Denzler, and Christoph Redies. 2014. JenAesthetics Subjective Dataset: Analyzing Paintings by Subjective Scores. In *ECCV Workshops*.
- [2] Seyed Ali Amirshahi, Gregor Uwe Hayn-Leichsenring, Joachim Denzler, and Christoph Redies. 2016. Color: A Crucial Factor for Aesthetic Quality Assessment in a Subjective Dataset of Paintings. *arXiv preprint arXiv:1609.05583* (2016).
- [3] Anurag Arnab, Mostafa Dehghani, Georg Heigold, Chen Sun, Mario Lucic, and Cordelia Schmid. 2021. ViViT: A Video Vision Transformer. In *ICCV, 2021*.
- [4] Gedas Bertasius, Heng Wang, and Lorenzo Torresani. 2021. Is Space-Time Attention All You Need for Video Understanding?. In *ICML, 2021*.
- [5] Yi Bin, Wenhao Shi, Yujuan Ding, Zhiqiang Hu, Zheng Wang, Yang Yang, See-Kiong Ng, and Heng Tao Shen. 2024. GalleryGPT: Analyzing Paintings with Large Multimodal Models. In *MM, 2024*.
- [6] Marion Botella and Todd Lubart. 2016. *Creative Processes: Art, Design and Science*.
- [7] Marion Botella, Franck Zenasni, and Todd Lubart. 2018. What Are the Stages of the Creative Process? What Visual Art Students Are Saying. *Frontiers in Psychology* (2018).
- [8] Marion Botella, Franck Zenasni, Julien Nelson, and Todd Lubart. 2022. Creative Processes in Five Domains: Art, Design, Scriptwriting, Music and Engineering. In *Homo Creativus: The 7 C's of Human Creativity*.
- [9] Gustavo Carneiro, Nuno Pinho da Silva, Alessio Del Bue, and João Paulo Costeira. 2012. Artistic Image Classification: An Analysis on the PRINTART Database. In *ECCV, 2012*.
- [10] João Carreira and Andrew Zisserman. 2017. Quo Vadis, Action Recognition? A New Model and the Kinetics Dataset. In *CVPR, 2017*.
- [11] Bowei Chen, Yifan Wang, Brian Curless, Ira Kemelmacher-Shlizerman, and Steven M. Seitz. 2024. Inverse Painting: Reconstructing The Painting Process. In *SIGGRAPH Asia, 2024*.
- [12] Marcos V. Conde and Kerem Turgutlu. 2021. CLIP-Art: Contrastive Pre-Training for Fine-Grained Art Classification. In *CVPR Workshops, 2021*.
- [13] DeepSeek-AI. 2024. DeepSeek-V3 Technical Report. *arXiv preprint arXiv:2412.19437* (2024).
- [14] Alexey Dosovitskiy, Lucas Beyer, Alexander Kolesnikov, Dirk Weissenborn, Xiaohua Zhai, Thomas Unterthiner, Mostafa Dehghani, Matthias Minderer, Georg Heigold, Sylvain Gelly, Jakob Uszkoreit, and Neil Houlsby. 2021. An Image is Worth 16x16 Words: Transformers for Image Recognition at Scale. In *ICLR, 2021*.
- [15] William Fedus, Barret Zoph, and Noam Shazeer. 2022. Switch Transformers: Scaling to Trillion Parameter Models with Simple and Efficient Sparsity. *J. Mach. Learn. Res.* (2022).
- [16] Christoph Feichtenhofer, Haoqi Fan, Jitendra Malik, and Kaiming He. 2019. Slow-Fast Networks for Video Recognition. In *ICCV, 2019*.
- [17] Anna Fekete, Matthew Pelowski, Eva Specker, David Briber, Raphael Rosenberg, and Helmut Leder. 2022. The Vienna Art Picture System (VAPS): A Data Set of 999 Paintings and Subjective Ratings for Art and Aesthetics Research. *Psychology of Aesthetics, Creativity, and the Arts* (2022).
- [18] Noa Garcia and George Vogiatzis. 2018. How to Read Paintings: Semantic Art Understanding with Multi-modal Retrieval. In *ECCV Workshops*.
- [19] Kaiming He, Xiangyu Zhang, Shaoqing Ren, and Jian Sun. 2016. Deep Residual Learning for Image Recognition. In *CVPR, 2016*.
- [20] Gao Huang, Zhuang Liu, Laurens van der Maaten, and Kilian Q. Weinberger. 2017. Densely Connected Convolutional Networks. In *CVPR, 2017*.
- [21] Zhewei Huang, Wen Heng, and Shuchang Zhou. 2019. Learning to paint with model-based deep reinforcement learning. In *ICCV, 2019*.
- [22] Shiqi Jiang, Ning Li, Chen Shi, Liping Guo, Changbo Wang, and Chenhui Li. 2024. AAPC: Aesthetics Assessment of Children's Paintings Based on Self-Supervised Learning. In *AAAI, 2024*.
- [23] Xin Jin, Qianqian Qiao, Yi Lu, Huaye Wang, Shan Gao, Heng Huang, and Guangdong Li. 2024. Paintings and Drawings Aesthetics Assessment with Rich Attributes for Various Artistic Categories. In *IJCAI, 2024*.
- [24] Xin Jin, Qianqian Qiao, Yi Lu, Huaye Wang, Heng Huang, Shan Gao, Jianfei Liu, and Rui Li. 2024. APDDv2: Aesthetics of Paintings and Drawings Dataset with Artist Labeled Scores and Comments. In *NeurIPS, 2024*.
- [25] C. Richard Johnson, Ella Hendriks, Igor J. Bereznoy, Eugene Brevdo, Shannon M. Hughes, Ingrid Daubechies, Jia Li, Eric Postma, and James Z. Wang. 2008. Image processing for artist identification. *IEEE Signal Processing Magazine* (2008).
- [26] Shuqi Liu, Jia Bu, Huayuan Ye, Juntong Chen, Shiqi Jiang, Mingtian Tao, Liping Guo, Changbo Wang, and Chenhui Li. 2024. DoodleTunes: Interactive Visual Analysis of Music-Inspired Children Doodles with Automated Feature Annotation. In *CHI, 2024*.
- [27] Songhua Liu, Tianwei Lin, Dongliang He, Fu Li, Ruifeng Deng, Xin Li, Errui Ding, and Hao Wang. 2021. Paint Transformer: Feed Forward Neural Painting with Stroke Prediction. In *ICCV, 2021*.
- [28] Ze Liu, Yutong Lin, Yue Cao, Han Hu, Yixuan Wei, Zheng Zhang, Stephen Lin, and Baining Guo. 2021. Swin Transformer: Hierarchical Vision Transformer using Shifted Windows. In *ICCV, 2021*.
- [29] Ze Liu, Jia Ning, Yue Cao, Yixuan Wei, Zheng Zhang, Stephen Lin, and Han Hu. 2022. Video Swin Transformer. In *CVPR, 2022*.
- [30] Hui Mao, Ming Cheung, and James She. 2017. DeepArt: Learning Joint Representations of Visual Arts. In *MM*.
- [31] Alibaba Group QwenTeam. 2025. Qwen2.5-VL Technical Report. *arXiv preprint arXiv:2502.13923* (2025).
- [32] Alec Radford, Jong Wook Kim, Chris Hallacy, Aditya Ramesh, Gabriel Goh, Sandhini Agarwal, Girish Sastry, Amanda Askell, Pamela Mishkin, Jack Clark, Gretchen Krueger, and Ilya Sutskever. 2021. Learning Transferable Visual Models From Natural Language Supervision. In *ICML, 2021*.
- [33] Aditya Ramesh, Prafulla Dhariwal, Alex Nichol, Casey Chu, and Mark Chen. 2022. Hierarchical Text-Conditional Image Generation with CLIP Latents. *arXiv preprint arXiv:2204.06125* (2022).
- [34] Robin Rombach, Andreas Blattmann, Dominik Lorenz, Patrick Esser, and Björn Ommer. 2022. High-Resolution Image Synthesis with Latent Diffusion Models. In *CVPR, 2022*.
- [35] Christoph Schuhmann, Romain Beaumont, Richard Vencu, Cade Gordon, Ross Wightman, Mehdi Cherti, Theo Coombes, Aarush Katta, Clayton Mullis, Mitchell Wortsman, Patrick Schramowski, Srivatsa Kundurthy, Katherine Crowson, Ludwig Schmidt, Robert Kaczmarczyk, and Jenia Jitsev. 2022. LAION-5B: An open large-scale dataset for training next generation image-text models. In *NeurIPS, 2022*.
- [36] Lior Shamir, Tomasz J. Macura, Nikita Orlov, D. Mark Eckley, and Ilya G. Goldberg. 2010. Impressionism, expressionism, surrealism: Automated recognition of painters and schools of art. *ACM Trans. Appl. Percept.* (2010).
- [37] Yiren Song, Shijie Huang, Chen Yao, Hai Ci, Xiaojun Ye, Jiaming Liu, Yuxuan Zhang, and Mike Zheng Shou. 2024. ProcessPainter: Learning to draw from sequence data. In *SIGGRAPH Asia, 2024*.
- [38] Gjorgji Strezoski and Marcel Worring. 2018. OmniArt: A Large-scale Artistic Benchmark. *ACM Trans. Multim. Comput. Commun. Appl.* (2018).
- [39] Jianlin Su, Murtadha H. M. Ahmed, Yu Lu, Shengfeng Pan, Wen Bo, and Yinfeng Liu. 2024. RoFormer: Enhanced transformer with Rotary Position Embedding. *Neurocomputing* (2024).
- [40] Wei Ren Tan, Chee Seng Chan, Hernán E. Aguirre, and Kiyoshi Tanaka. 2016. Ceci n'est pas une pipe: A deep convolutional network for fine-art paintings classification. In *ICIP, 2016*.
- [41] Llama Team. 2024. The Llama 3 Herd of Models. *arXiv preprint arXiv:2407.21783* (2024).
- [42] Paints-Undo Team. 2024. Paints-Undo GitHub Page.
- [43] Zhan Tong, Yibing Song, Jue Wang, and Limin Wang. 2022. VideoMAE: Masked Autoencoders are Data-Efficient Learners for Self-Supervised Video Pre-Training. In *NeurIPS, 2022*.
- [44] Hugo Touvron, Matthieu Cord, Matthijs Douze, Francisco Massa, Alexandre Sablayrolles, and Hervé Jégou. 2021. Training data-efficient image transformers & distillation through attention. In *ICML, 2021*.
- [45] Limin Wang, Bingkun Huang, Zhiyu Zhao, Zhan Tong, Yanan He, Yi Wang, Yali Wang, and Yu Qiao. 2023. VideoMAE V2: Scaling Video Masked Autoencoders with Dual Masking. In *CVPR, 2023*.
- [46] Victoria Yanulevskaya, Jasper R. R. Uijlings, Elia Bruni, Andreza Sartori, Elisa Zamboni, Francesca Bacci, David Melcher, and Nicu Sebe. 2012. In the eye of the beholder: employing statistical analysis and eye tracking for analyzing abstract paintings. In *MM*.
- [47] Ran Yi, Haoyuan Tian, Zhihao Gu, Yu-Kun Lai, and Paul L. Rosin. 2023. Towards Artistic Image Aesthetics Assessment: a Large-scale Dataset and a New Method. In *CVPR, 2023*.
- [48] Zhengxia Zou, Tianyang Shi, Shuang Qiu, Yi Yuan, and Zhenwei Shi. 2021. Stylized Neural Painting. In *CVPR, 2021*.